DOI: 10.1002/chem.201003634

Uptake of Liquid Alcohols by the Flexible Fe^{III} Metal–Organic Framework MIL-53 Observed by Time-Resolved In Situ X-ray Diffraction

Richard I. Walton,*[a] Alexis S. Munn,[a] Nathalie Guillou,[b] and Franck Millange[b]

Abstract: A comprehensive, time-resolved, energy-dispersive X-ray diffraction study of the uptake of liquid alcohols (methanol, ethanol, propan-1-ol and propan-2-ol) by the flexible metal-organic framework solid MIL-53(Fe)-[H_2O] is reported. In the case of the primary alcohols, a fluorinated version of the MIL-53(Fe) host (*C*2/*c* symmetry *V* ca. 1000 Å^3), in which a fraction of framework hydroxides are replaced by fluoride, shows uptake of alcohols to give initially a partially expanded phase (*C*2/*c* symmetry, *V* ca. 1200 Å^3) followed by an expanded form of the material (either *Imcm* or *Pnam* symmetry, *V* ca. 1600 Å^3). In the case of methanol–water mixtures, the EDXRD data show that the partially open intermediate phase undergoes volume expansion during its existence, before switching to a fully open structure if concentrated methanol is used; analogous behaviour is seen if the initial guest is propan-2-ol, which then is replaced by pyridine, where a continuous shift of Bragg peaks within *C*2/*c* symmetry is observed. In contrast to the partially fluorinated materials, the purely hydroxylated host materials show little tendency to stabilise partially open forms of MIL-53(Fe) with primary alcohols and the kinetics of guest introduction are markedly slower without the framework fluorination: this is exemplified by the exchange of water by propan-2-ol, where a partially open *C*2/*c* phase is formed in a step-wise manner. Our study defines the various possible pathways of liquid-phase uptake of molecular guests by flexible solid MIL-53(Fe).

Keywords: metal–organic frameworks · microporous materials · solid-state structures · X-ray diffraction · zeolite analogues

Introduction

Much research is currently focussed upon the synthesis, properties and applications of metal-organic framework (MOF) materials.[1] These are hybrid, inorganic–organic solids with extended structures constructed from metal centres linked by polydentate ligands that may present considerable porosity once solvent or excess organic ligand is removed from the structure after synthesis. Although the open structures of purely inorganic solids, such as zeolites and their analogues, have been well-studied for many years,[2] MOFs have brought significant novelty to the field of porous materials. There are a number of reasons for this, including the ease of modification of chemical and physical properties by choice of the ligand and metal combination,[3] the possibility of post-synthesis functionalisation of the organic components of structures to tune selectivity towards guest uptake[4] and the structural flexibility offered in hybrid materials over conventional inorganic networks.[5] These aspects of MOF chemistry offer new possibilities in the applications of porous materials[6] in important contemporary areas such as molecular separation and storage for environmental and energy applications,[7] shape-selective heterogeneous catalysis under mild conditions,[8] battery materials[9] and drug delivery.[10]

The remarkable flexibility of MOFs may involve displacement of atoms over several Ångströms whilst maintaining the connectivity of the three-dimensional structure, and indeed the crystallinity of the material.[5b] Examples include work by Kitagawa and co-workers[11] who have shown how gas sorption towards CO_2, N_2, O_2 etc. may be tuned by the structural flexibility offered by coordination polymers,[12] and recent work by Rosseinsky and co-workers on zinc peptide frameworks that show flexibility towards gas sorption resembling the conformational changes of proteins.[13] It is apparent that with this structural flexibility MOFs offer the possibility as highly tunable and selective molecular sieves.[5] Particularly striking is the case of metal carboxylates belonging to the MIL-*n* (MIL = Material of Institut Lavoisier) family: for example the structurally related phases MIL-88 and MIL-89 show a solvent-dependent swelling that may achieve a 300% increase in unit cell volume,[14] while MIL-53 shows two-dimensional flexibility that reflects the relatively rigid one-dimensional inorganic chains that form the backbone of its structure.[15] This phenomenon of reversible volume expansion has been described as 'breathing' and the property has been rationalised by considering local flexibility of the structures.[5b] Materials with the MIL-53

[a] Dr. R. I. Walton, A. S. Munn
Department of Chemistry, University of Warwick
Coventry, CV4 7AL (UK)
Fax: (+44) 2476 524112
E-mail: r.i.walton@warwick.ac.uk

[b] Dr. N. Guillou, Dr. F. Millange
Institut Lavoisier Versailles, Université de Versailles
UMR 8180, 78035 Versailles (France)

Supporting information for this article is available on the WWW under http://dx.doi.org/10.1002/chem.201003634.

structure have now been studied extensively for their vapour phase sorption properties, and they show high capacity for a variety of small molecules including CO_2, H_2, H_2S and hydrocarbons, where in some cases an evolution of structure with guest concentration has been observed.[16] It has also been noted that the behaviour of the various structural analogues of MIL-53, where the framework trivalent metal ion is varied from Cr, Fe, Al, or Ga, is rather different: for example in its dehydrated state MIL-53(Cr) has a fully open structure, but for dehydrated MIL-53(Fe) the structure is closed,[15c] and while the thermal behaviour of the aluminium analogue is similar to the chromium material, the gallium material behaves differently with the closed form persisting to higher temperature.[17]

To learn more about the mechanism of flexibility of MIL-53 materials we herein describe a comprehensive, time-resolved in situ diffraction study of the interaction of iron(III) containing MIL-53 solids with a series of simple alcohols, methanol, ethanol, propan-1-ol and propan-2-ol, in the liquid phase. This work follows from a preliminary communication in which we reported the observation of a crystalline intermediate in the case of methanol sorption from the liquid phase,[18] suggesting that the pore-opening associated with breathing may be a complex process involving several steps. We have now extended our study to a range of other alcohols and also at the same time investigated the simplest modification of the MIL-53 structure: the partial replacement of framework hydroxide by fluoride. The use of the energy-dispersive X-ray diffraction (EDXRD) method has uniquely allowed monitoring of the uptake of a liquid-phase guest by a solid on a laboratory scale since the combination of the intense, white X-ray beam and the fixed-angle, solid-state detector means that rapid data collection is possible from crystalline solids in bulky reaction vessels. This is particularly advantageous in the case of solid–liquid reactions since heterogeneous reaction mixtures can be studied without problems of reproducibility that may occur upon scaling down: this has been illustrated previously in a variety of situations including hydrothermal and solvothermal crystallisation of various inorganic materials and minerals, and the solution-mediated intercalation chemistry of layered solids.[19] Thus, despite the inherent low energy resolution of the energy-discriminating detector, the EDXRD method permits the temporal evolution of crystalline phases to be determined in reacting heterogeneous mixtures to yield unprecedented insight into crystallisation events.

Results and Discussion

Characterisation of the MIL-53(Fe)[guest] materials: The structure of hydrated MIL-53(Fe)[H_2O] has already been described in both hydroxylated, $Fe^{III}(OH)(O_2C\text{-}C_6H_4\text{-}CO_2).(H_2O)$,[15c] and partially fluorinated, $Fe^{III}(OH)_{0.8}F_{0.2}(O_2C\text{-}C_6H_4\text{-}CO_2).(H_2O)$[20] variants. For simplification we will now refer to these materials as MIL-53(Fe,OH)[H_2O] and MIL-53(Fe,F,OH)[H_2O], respectively. The two solids have essentially identical structures, Figure 1a and b, but the former has a superstructure not seen in the fluorinated material which in turn gives two unique lozenge-shaped channels

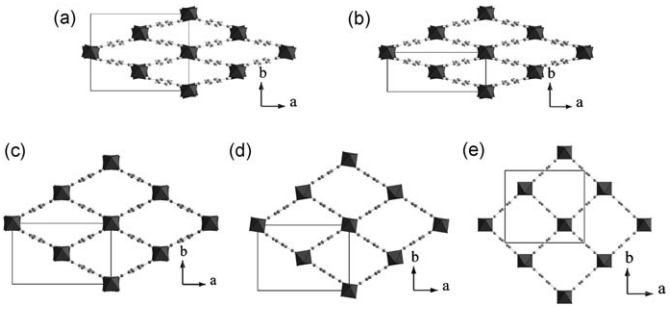

Figure 1. The structure of MIL-53(Fe) in various expanded forms showing the relationship of unit cell volume to the framework topology. (a) Closed $P2_1/c$ form seen for MIL-53(Fe,OH)[H_2O],[15c] (b) closed $C2/c$ form seen for MIL-53(Fe,F,OH)[H_2O],[20] (c) partially open $C2/c$ form seen for MIL-53(Fe,F,OH)[pyridine][20] and for the case where diluted alcohols are added, (d) open *Pnam* form seen in the presence of excess propan-1-ol and (e) fully open *Imcm* form seen in the presence of excess methanol or ethanol. Guest molecules are omitted. See Table 1 for unit cell parameters of the materials studied in the present work.

rather than one, although the guest water molecules interact with the framework in a similar manner through hydrogen bonding with the bridging OH that forms the backbone of the inorganic chains, and also with another water molecule to form pairs.[15c] Table 1 shows refined unit cells for all of the materials MIL-53(Fe)[guest] studied: these define the structures of the solids in the presence of solvent in their equilibrium state, that is, after being immersed in excess solvent for several hours. Figure 1 shows the relationship between the various crystal symmetries encountered and the basic MIL-53 structure type: the topology of the framework is identical in each case, but small structural distortions result in various crystal symmetries. In most cases, the effect of framework fluorination is subtle, but detectable in small changes in unit cell volume: in general the fluorinated host material has a slightly smaller unit cell volume than the fully hydroxylated material for a given guest.

Uptake of methanol by MIL-53(Fe)[H_2O]: Our first aim in the study of the interaction of MIL-53 with alcohols was to clarify the observation of an intermediate crystalline phase during the interaction of pure methanol with a suspension of solid MIL-53(Fe,F,OH)[H_2O] in water.[18] Figure 2 shows contour maps of the uptake of methanol as three dilutions in water. The final product of the reaction using pure methanol, Figure 2a, matches the material produced upon immersing the solid in methanol for several hours and has a fully open structure (*Imcm* symmetry; see Table 1, and the Supporting Information for assignment of EDXRD), but that there is clear evidence for a transient, crystalline intermediate. Figure 2b and c show that if the MeOH is diluted with water then the crystalline transient phase appears for longer periods of time, and indeed if a 50:50 (by volume) of

Table 1. Unit cell parameters and symmetries for MIL-53(Fe)[guest] compounds. Unit cell edges have units of Å and angles units of degrees.

Guest	MIL-53(Fe,OH)[guest]		MIL-53(Fe,OH,F)[guest]	
H_2O closed form	$P2_1/c$ Ref. [15c]	$a=19.3197(2)$ $b=15.0362(2)$ $c=6.83508(6)$ $\beta=96.305(1)$ $V=1973.55(3)$	$C2/c$ Ref. [20]	$a=21.1299(1)$ $b=7.64271(6)$ $c=6.83058(6)$ $\beta=114.9352(4)$ $V=1000.25(2)$
MeOH fully open form	*Imcm*	$a=15.9557(5)$ $b=14.4534(4)$ $c=6.9270(2)$ $V=1597.47(7)$	*Imcm*	$a=15.9394(3)$ $b=14.4526(3)$ $c=6.90489(8)$ $V=1590.65(5)$
MeOH intermediate form[a]	Not observed		$C2/c$	$a=20.5463(1)$ $b=9.17002(8)$ $c=6.87319(6)$ $\beta=112.9817(6)$ $V=1192.19(2)$
EtOH fully open form	*Imcm*	$a=15.9988(4)$ $b=14.4422(3)$ $c=6.90410(6)$ $V=1595.24(5)$	*Imcm*	$a=16.2079(2)$ $b=14.1441(2)$ $c=6.89163(3)$ $V=1579.87(3)$
EtOH intermediate form[a]	Not observed		$C2/c$	$a=20.5127(2)$ $b=9.2468(2)$ $c=6.87361(9)$ $\beta=113.1070(9)$ $V=1199.16(3)$
1-PrOH fully open form	*Pnam* *Imcm* (minor)[b]	$a=16.7029(3)$ $b=13.2526(2)$ $c=6.90750(6)$ $V=1529.02(3)$ $a=17.1668(2)$ $b=12.7803(2)$ $c=6.90064(9)$ $V=1513.97(3)$	*Imcm*	$a=17.1382(2)$ $b=12.7876(2)$ $c=6.89262(4)$ $V=1510.56(3)$
1-PrOH intermediate form[a]	Not observed		$C2/c$	$a=20.3420(2)$ $b=9.63570(7)$ $c=6.87980(6)$ $\beta=112.8406(5)$ $V=1242.77(2)$
2-PrOH	$C2/c$	$a=20.1997(2)$ $b=10.05281(9)$ $c=6.88674(6)$ $\beta=112.9658(7)$ $V=1287.61(2)$	$C2/c$	$a=20.2269(1)$ $b=9.9400(2)$ $c=6.87300(4)$ $\beta=113.0698(4)$ $V=1271.34(2)$
pyridine	Not studied		$C2/c$ Ref. [20]	$a=19.2034(2)$ $b=11.1758(1)$ $c=6.88903(6)$ $\beta=109.0041(6)$ $V=1397.89(3)$

[a] As discussed in the text the 'intermediate' forms were isolated by immersion of the solid host in alcohol diluted with water. [b] $<5\,\%$ by mass.

water/methanol mixture is added to MIL-53(Fe,F,OH)[H_2O] then the sole product after six hours is only the 'intermediate' phase. With this knowledge, the use of high resolution powder XRD from a solid produced by immersing MIL-53-(Fe,F,OH)[H_2O] in 50 % methanol solution in water allowed successful indexing of this phase as having $C2/c$ symmetry and a unit cell volume close to the average of the 'closed' hydrated phase and the 'fully open' phase present after immersing the solid in pure methanol (Table 1). Determination of Bragg peak areas as a function of time in the EDXRD experiment allowed extent of reaction curves to be produced (Figure 3).[21] At 75 % dilution, (Figure 3b), the curves reveal the relationship between the growth and decay of the intermediate phase and that of the final product: once the intermediate phase has decayed (ca. 340 min), the growth of the final product accelerates. Note that in the most dilute case, (Figure 3c), the Bragg peak intensities of the intermediate phase (the sole product) gradually decay. This may be due to several factors, including dilution of the system by the large volume of liquid added at this point, or a settling of the solid in this long experiment; nevertheless, there is no trace of the fully open *Imcm* product. It is important to note that the partially open $C2/c$ form is formed in a 'step-wise' manner from the closed hydrated $C2/c$ form and subsequently the fully open *Imcm* phase is formed in the same way: the phases coexist for a period rather than one evolving into the other. The same situation was seen previously for the uptake of other organics from the liquid phase, including pyridine, 2,6-lutidine and *m*-xylene.[18,20]

A closer inspection of the EDXRD data reveals additional information about the partially open material, not apparent from the static study. During the lifetime of the phase the Bragg peaks shift in a concerted manner, thus indicating a changing unit cell volume with time. Given the monoclinic unit cell and the small total number of independent observed Bragg peaks (only eight peaks can be defined unambiguously), it is not

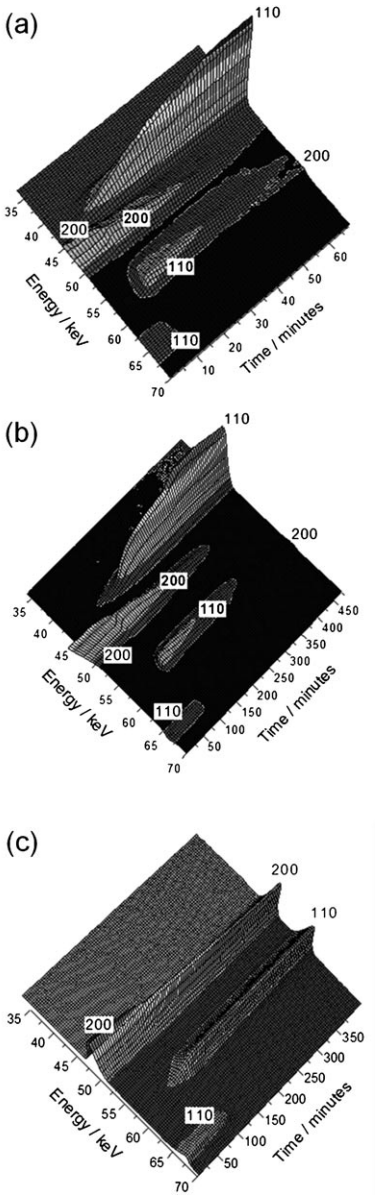

Figure 2. Contour maps of EDXRD measured during the addition of methanol/water to MIL-53 MIL-53(Fe,F,OH)[H_2O]. (a) Pure methanol, (b) 75% methanol in water and (c) 50% methanol in water. The syringe pump speed was constant for each of these experiments (1 mL per hour) and the detector angle was set at 1.495 °2θ. Miller indices were assigned by using the lattice parameters measured by high-resolution powder XRD (Table 1); those of the intermediate phase are shown in grey.

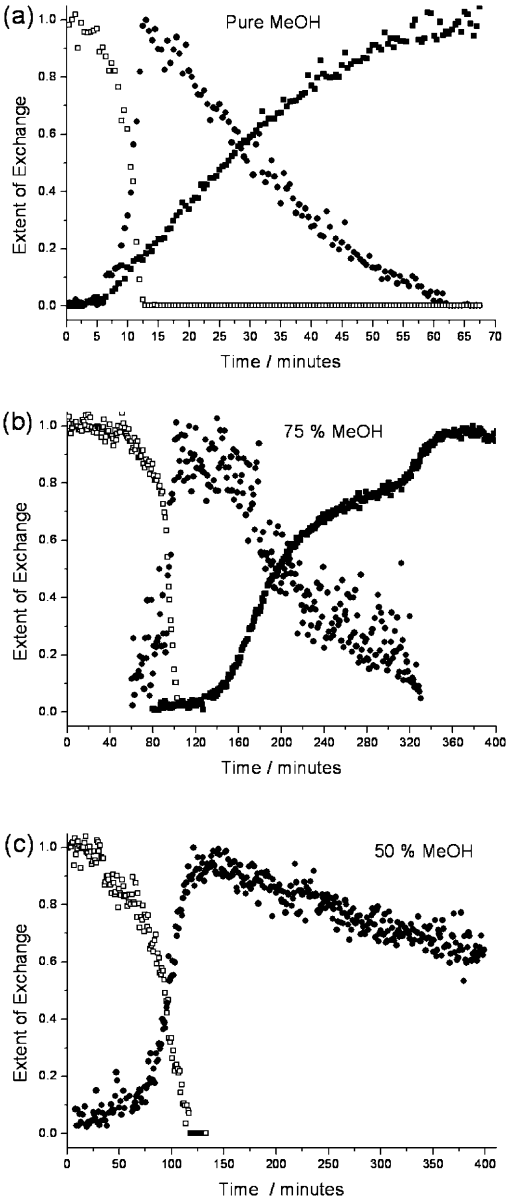

Figure 3. Normalised integrated Bragg peak intensities of MIL-53-(Fe,F,OH)[H_2O] (110 peak, open squares), partially open intermediate (110 peak, circles) and fully open product (110 peak, squares) in the presence of (a) pure methanol, (b) 75% methanol in water and (c) 50% methanol in water.

possible to refine a unit cell from the EDXRD data, and so the positions of the three strongest selected signals are plotted on Figure 4a–c. It can be seen how the (200) and (110) peaks shift in opposite directions: this is consistent with a contraction of the *a* axis and an expansion of the *b* axis. The changing geometry and overall unit cell expansion with time is indicated on Figure 4d. The curves have a distinctive shape with an initial rapid expansion along *b* when the phase first forms which then slows (note that for the (200) peak it overlaps with the decaying starting phase (200) peak so its position is only plotted from the time when it exists alone). The final values of peak positions in this experiment approach those seen for the material produced upon equilibration of a sample with a 50-50 water-methanol mixture (Table 1), suggesting an upper limit to the volume of this partially open phase. In this longer in situ EDXRD experiment we could also monitor the Bragg peak positions of the initial MIL-53(Fe,F,OH)[H_2O] during its decay, and here we do see a shift to higher *d*-spacing of the (110) peak, suggesting a cell expansion prior to the switch to the partially open material, but this is an order of magnitude smaller than for the changes seen during the lifetime of the transient, partially open material (see the Supporting Information).

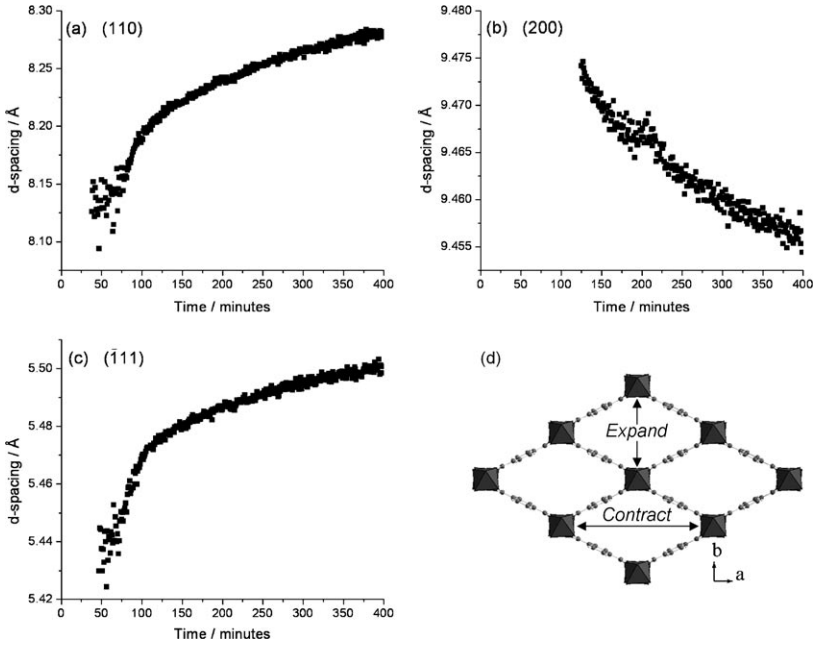

Figure 4. Plots of Bragg peak position of the partially open intermediate phase seen during addition of 50% MeOH in water to MIL-53(Fe,F,OH) for (a) the (110) peak, (b) the (200) peak and (c) the (−111) peak. (d) An illustration of the structural transformation during this process.

Although we were able to isolate the partially intermediate phase in a capillary by using diluted methanol and determine its lattice parameters, a full structure solution from the high-resolution powder X-ray diffraction data has not proved possible. An attempt at structure solution reveals the inorganic–organic framework, but the Fourier difference maps do not resolve fully occupied sites for the guest molecules, suggesting considerable disorder in their location. It is also not clear from crystallography whether the guest molecules at this point are purely methanol or a mixture of water and methanol. However, the fact that the material is isolated in diluted methanol would suggest the presence of a mixture of two guest molecules: the fact that the material undergoes a volume expansion during its existence can then be explained by a continuous adjustment of the composition of the mixture of guest molecules up to a limit where the partially open phase reaches its maximum volume and then transforms to a fully open structure.

An effect of fluorination of the host on methanol uptake is apparent. The intermediate, partially-open form is rather difficult to detect when the pure hydroxylated material, MIL-53(Fe,OH)[H_2O], is used as the host, and even when the methanol is diluted, the Bragg peaks of the partially open phase are very weak and appear alongside the fully open product (see the Supporting Information). This immediately suggests some difference in sorption behaviour between the pure hydroxylated and fluorinated host. This will be discussed further below for the case of other alcohols, where the difference is more obvious.

Uptake of ethanol by MIL-53(Fe)[H_2O]: Figure 5a shows the EDXRD spectra measured during the uptake of ethanol by MIL-53(Fe,F,OH)[H_2O] without dilution by extra water. At a glance, this shows direct transformation to the 'fully open' *Imcm* product, but a closer inspection reveals the presence of a small amount of a transient phase, represented by a shoulder on the product (200) peak. Dilution to 75% in water, Figure 5b, prolongs the lifetime of the intermediate slightly, but the phase is not observed in a pure form without further dilution and also slowing of the speed of addition of the liquid to the suspension, Figure 5c and d. This clearly shows how the intermediate phase is a kinetic product that can be isolated by adjusting either the dilution or the rate of addition of the guest molecules. With this knowledge we were able subsequently to isolate the intermediate phase in a capillary for high-resolution powder X-ray diffraction: it is identified as a *C*2/*c* partially open form (see Table 1). The two phases seen by EDXRD (partially open and then fully open) match the lattice parameters derived from the high resolution study (Table 1), confirming their unit cell volumes. Figure 6 shows the results of integrated peak areas during ethanol uptake. These reveal some new information: with slow addition of the guests, for example 100% ethanol at 1 mL per hour the formation of an expanded phase is not observed until a critical volume of guest is added to the suspension: there is a distinct induction time before the product is detected. This is in contrast to our previous observations of the uptake of molecules such as pyridine, 2,4-dimethylpyridine and *o*-xylene,[18,20] where the formation of an expanded form of MIL-53(Fe) was observed immediately upon addition of the smallest amount of the pure liquid guest. This suggests that the solution composition is crucial for the swelling of MIL-53(Fe) by ethanol, in turn implying that the guest species are a mixture of alcohol and water rather than being pure alcohol. This is backed by another observation: if the ethanol is diluted to 10% by volume in water no swelling of the solid occurs even after prolonged immersion in the liquid ($>$ 15 h). As with the case of methanol, the intermediate, partially open material shows a volume expansion during its existence, as shown by a shift of the (110) peak position up to a maximum value (see the Supporting Information). The behaviour of MIL-53(Fe,OH)[H_2O] is in contrast to its fluorinated analogue in that we only ever observe the formation of the fully expanded product and never an intermediate, partially open phase; furthermore there is a marked reduction in kinetics of ex-

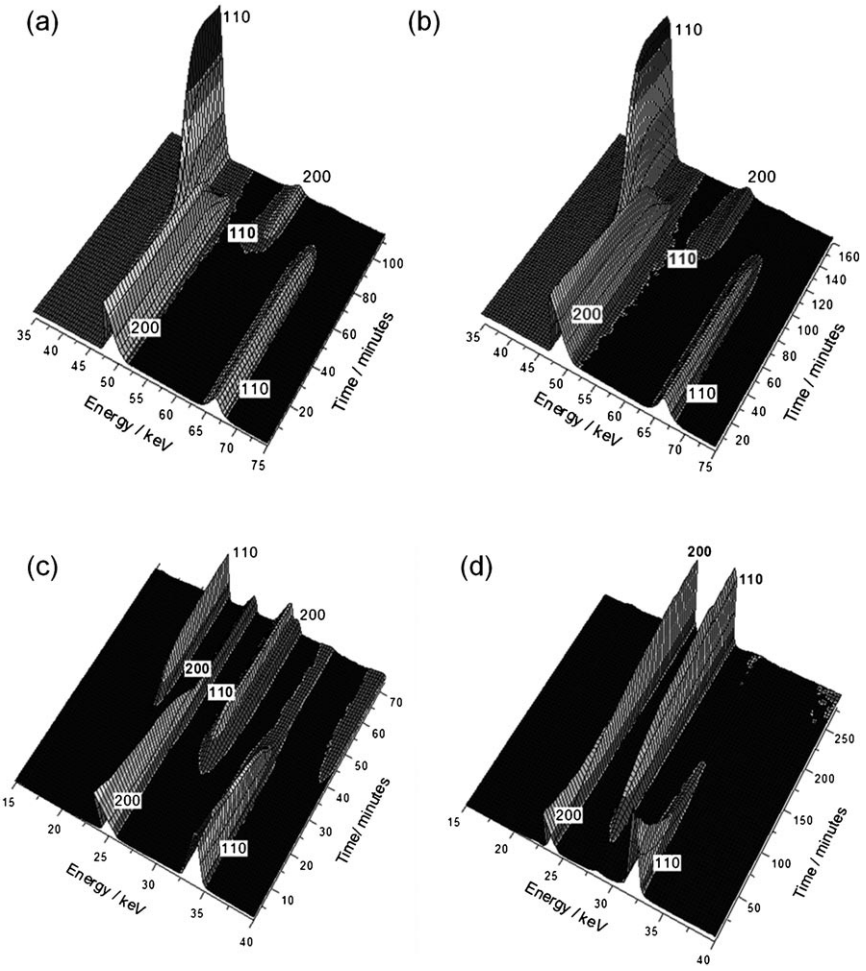

Figure 5. Contour maps of EDXRD measured during the addition of ethanol/water to MIL-53 MIL-53-(Fe,F,OH)[H_2O]. (a) Pure ethanol at 1 mL per hour, (b) 75% ethanol in water at 1 mL per hour, (c) 25% ethanol in water at 10 mL per hour and (d) 25% ethanol in water at 5 mL per hour. The detector angle was set at 1.50 °2θ in (a) and (b), at 2.92 °2θ in (c) and at 3.05 °2θ in (d). Note that the data in (a) and (b) were recorded using Station 16.4 while those in (c) and (d) were measured on Beamline F3 so the incident energy ranges differ. Miller indices were assigned by using the lattice parameters measured by high-resolution powder XRD (Table 1); those of the intermediate phase are shown in grey.

change when the host contains no fluorine (see the Supporting Information).

Uptake of propanols by MIL-53(Fe)[H_2O]: The case of uptake of propan-1-ol by MIL-53(Fe)[H_2O] is rather similar to the behaviour in the presence of ethanol. The fluorinated precursor, MIL-53(Fe,F,OH)[H_2O] takes up the guest through a partially open crystalline intermediate (Figure 7a), whose lifetime may be prolonged by dilution combined with slow addition of the liquid host (see the Supporting Information). In contrast, the hydroxylated precursor, MIL-53(Fe,OH)[H_2O] produces the fully expanded product directly (Figure 7b). These observations are consistent with the high resolution powder XRD study (Table 1). The case of propan-2-ol is rather different since the product formed on equilibration in pure propan-2-ol for either the fluorinated or hydroxylated precursor has a structure with an intermediate unit cell volume (Table 1), rather than the fully expanded form of the material seen ultimately with propan-1-ol, Figure 7c and d. The in situ EDXRD data show that for both fluorinated and hydroxylated hosts, propan-2-ol is taken up directly in one step. The integrated peak intensities, however, show that the kinetics of exchange are rather different in each case (Figure 8). For the fluorinated host, guest exchange takes place more rapidly for both propanol isomers whether or not an intermediate phase is seen: the pure hydroxylated host decays in approximately double the time than for the partially fluorinated material if all other experimental factors are fixed (speed of stirring, rate of syringe pump etc.).

The possibility of separation of the two propanol isomers was also studied: Figure 9 shows the results of EDXRD analysis of the case when a 50:50 mixture of propan-1-ol and propan-2-ol is added to MIL-53(Fe,F,OH)[H_2O] in water. The first change seen is the appearance of the characteristic Bragg peaks of the MIL-53(Fe,F,OH)[propan-2-ol] material and these are soon followed by the appearance of Bragg peaks of MIL-53-(Fe,F,OH)[propan-1-ol] which grow at the expense of the propan-2-ol-containing material initially formed. The latter phase is not completely consumed, and this was the case for repeated experiments at the beamlines. It is interesting to note that the partially open MIL-53(Fe,F,OH)[propan-1-ol] is not seen: the unit cell volumes of this phase and the MIL-53-(Fe,F,OH)[propan-2-ol] material are sufficiently different to allow them to be distinguished (Table 1). The separation behaviour we see here is analogous to the situation where a mixture of pyridine and 2,6-lutidine is added to MIL-53-(Fe,F,OH)[H_2O]: the partially open pyridine phase is first seen and decays as the fully open 2,6-lutidine containing material is produced.[20] We therefore conclude that the tendency is to form the fully open form of MIL-53(Fe) if an excess of appropriate guest molecules is added in the liquid phase. This may potentially be exploited to separate mixtures of two molecules as the solid phase containing one guest may easily be recovered by filtration.

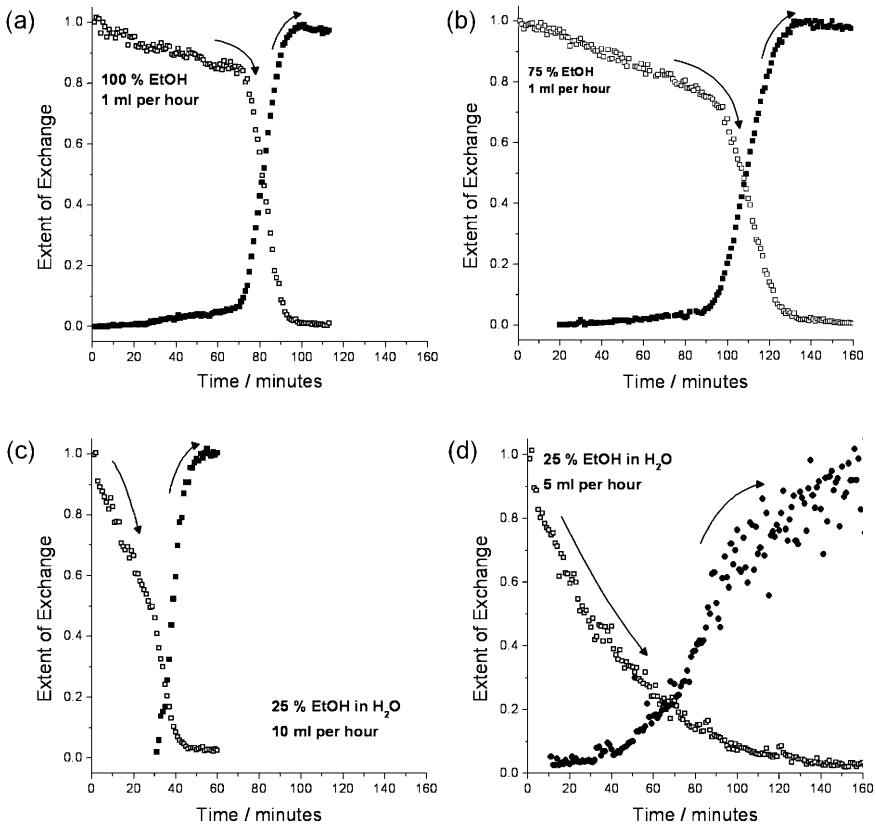

Figure 6. Normalised integrated Bragg peak intensities of MIL-53(Fe,F,OH)[H_2O] (110 peak, open squares), partially open intermediate (110 peak, circles) and fully open product (110 peak, squares) in the presence of (a) pure ethanol with an addition rate of 1 mL per hour, (b) 75% ethanol in water at 1 mL per hour, (c) 25% ethanol in water at 10 mL per hour and (d) 25% ethanol in water at 5 mL per hour.

Uptake of pyridine by MIL-53(Fe)[propan-2-ol]: The unit cell volumes of MIL-53(Fe,F,OH)[propan-2-ol] and MIL-53-(Fe,F,OH)[pyridine] are rather similar and they have identical crystal symmetry (Table 1) so it was of interest to study the exchange of one of these guests by the other, to contrast with the situations described above, in which the initial and final materials have rather different unit cell volumes. Therefore we prepared MIL-53(Fe,F,OH)[propan-2-ol] by stirring MIL-53(Fe,F,OH)[H_2O] in excess propan-2-ol and then added, dropwise, a 10% solution of pyridine in propan-2-ol to the suspension. Figure 10a and b show the EDXRD data measured using two different banks of data on Station 16.4, revealing that the uptake of pyridine occurs gradually with a continuous shift of the Bragg peak positions from starting material to product. In this case the extent of reaction can be determined by the progress of the shifting Bragg peak positions (because their area remains approximately constant): Figure 10c shows this result. All the signals show a shift to larger *d*-spacing during the exchange, which is consistent with the expansion of the unit cell volume from 1287.61(2) $Å^3$ to 1397.89(3) $Å^3$ (note that as we can only resolve Bragg peaks with Miller indices (h, $[k=h]$, l) and the c parameter remains similar, all peaks shift by the same relative amount). This 'continuous breathing' resembles the behaviour of the partially open intermediate seen in the case of dilute methanol discussed above, in this case between two unit cell volume limits defined by each of the pure guest molecules.

Conclusion

The uptake of simple liquid alcohols by hydrated MIL-53(Fe) leads to dramatic expansion (breathing) of the material, which has previously been seen in the presence of aromatic molecules such as pyridine and xylenes, and in the gas-phase sorption of small molecules in the chromium analogue MIL-53(Cr). In the case of primary alcohols this leads ultimately to a fully expanded version of MIL-53(Fe), whereas with the secondary alcohol propan-2-ol the final product has a partially expanded framework. Several key observations may be made about the pathways of exchange of the guest molecules in this system:

(1) If the unit cell volume change between the initial hydrated state and final host and the guest material is relatively large (ca. 150 $Å^3$), then the starting phase and final product co-exist as separate phases for a period: the exchange occurs in a step-wise fashion rather than evolution of one phase into another; for example, the exchange of water by propan-2-ol.

(2) Transformation from a closed (*C*2/*c*) to fully open (*Imcm*) framework (which always involves a volume change of $>$ 200 $Å^3$) may involve a transient intermediate partially open phase (also *C*2/*c* symmetry). This is stabilised for the host that is partially fluorinated, allowing it to be isolated if the alcohol is diluted; for example, the exchange of water by methanol, ethanol or propan-1-ol.

(3) If the volume change upon guest exchange is small ($<$150 $Å^3$) within the same crystal symmetry then continuous evolution of the structure may be seen; for example, the intermediate phase seen in methanol uptake or the exchange of propan-2-ol by pyridine.

(4) The purely hydroxylated framework behaves differently than the partially fluorinated host, with noticeably retarded kinetics of exchange (e.g., water by propan-2-ol) and the absence of partially open intermediates observed in the case of primary alcohols.

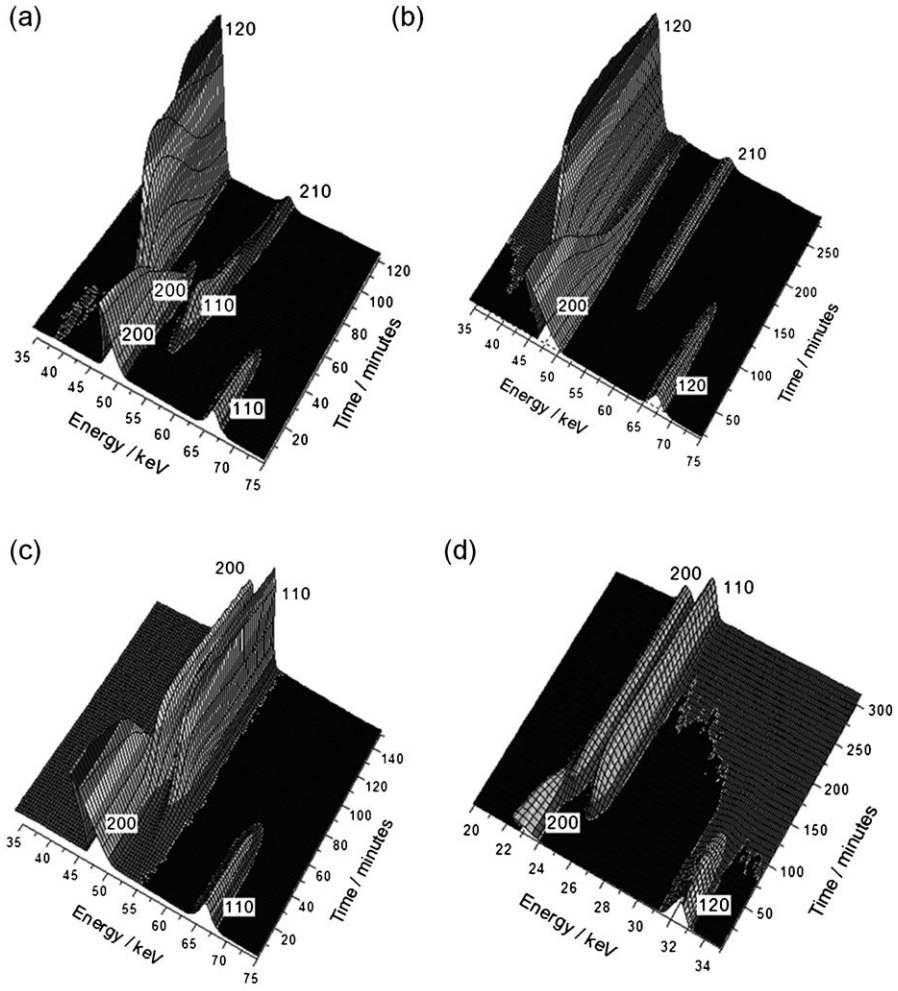

Figure 7. Contour maps of EDXRD measured during the addition of propanols to MIL-53(Fe). (a) Pure propan-1-ol into MIL-53(Fe,F,OH)[H_2O], (b) pure propan-1-ol into MIL-53 MIL-53(Fe,OH)[H_2O], (c) pure propan-2-ol into MIL-53 MIL-53(Fe,F,OH)[H_2O] and (d) pure propan-2-ol into MIL-53 MIL-53(Fe,OH)-[H_2O]. The syringe pump speed was constant for each of these experiments (1 mL per hour) and the detector angle was set at 1.50 °2θ, except in (d) where Beamline F3 was used with an angle of 3.05 °2θ. Miller indices were assigned by using the lattice parameters measured by high-resolution powder XRD (Table 1); those of the intermediate phase are shown in grey.

It is difficult to provide at present a complete explanation for the effect on the breathing property of fluoride inclusion in the MIL-53(Fe) structure, but for the materials whose full crystal structures are known it is apparent that host–guest interactions hold the key. For example, for the hydrated starting materials their crystal structures[15c,20] show the presence of hydrogen bonding between the guest water molecules and the framework OH/F that makes up the backbone of the infinite inorganic chains. The same is true for the material that contains pyridine, where N–HO hydrogen bonding is present.[20] Assuming that the hydroxide acts as a hydrogen-bond donor (as must be the case for pyridine, for example), then partial replacement of the hydroxide by fluoride will lessen the total host–guest hydrogen-bonding interactions. The effect may then be a more flexible framework that can interact with guests more readily and adapt to various combinations of mixtures of guest molecules. This is consistent with the faster kinetics of guest uptake we have seen for the fluorinated MIL-53(Fe) and also the stabilisation of partially open intermediate phases, which are likely to contain varying quantities of water and alcohol.

The important outcome of this study is that we defined the various behaviours of the flexible solid MIL-53(Fe) in the presence of liquid–phase organic guests, something that will be important in investigating the separation of more complex organic molecules for practical application. Clearly, the location of the alcohol guest molecules, which are crystallographically highly disordered, would help to further explain the new observations we have made. We suggest that spectroscopic studies may be helpful in this respect and this will be the focus of our future work.

Experimental Section

Preparation of MIL-53(Fe) in pure hydroxylated and partially fluorinated forms: MIL-53(Fe)[H_2O] was synthesised using a solvothermal method (autogenous pressure) from an equimolar amount of iron(III) chloride hexahydrate $FeCl_3.6H_2O$ (Aldrich, 97%, 1 mmol), 1,4-benzenedicarboxylic acid HO_2C-(C_6H_4)-CO_2H (Alfa, 97%, 1 mmol), in *N*,*N*′-dimethylformamide (DMF, Aldrich 99%, 5 mL). Reactants were stirred for a few minutes before introducing the resulting suspension in a Teflon-lined steel autoclave and the temperature was set at 423 K for three days. The light orange MIL-53(Fe)[DMF] powder was first washed with MeOH to obtain MIL-53(Fe)[MeOH] after complete exchange of DMF molecules by MeOH. Finally, MIL-53(Fe)[H_2O] was obtained after dispersion into water and drying in air. For the preparation of the fluorinated version of the solid host an equimolar amount of hydrofluoric acid HF (Prolabo, 5 M, 1 mmol) was also added to the reaction mixture before the solvothermal reaction. Quantitative elemental analyses for the fluorinated phase calcd (%) for $Fe^{III}(OH)_{0.8}F_{0.2}(O_2C$-$C_6H_4$-$CO_2).(H_2O)$: Fe 21.9, C 37.6, H 2.68 F 1.48; found: Fe 23.7, C 35.6, H 2.68, F 1.31. Quantitative elemental analyses for the purely hydroxylated phase calcd (%) for $Fe^{III}(OH)(O_2C$-C_6H_4-$CO_2).H_2O$: Fe 21.9, C 37.7, H 2.77; found: Fe 21.9, C 36.4; H 2.79, F <0.2. Laboratory powder X-ray diffraction, infrared spectroscopy and thermodiffractometry were also used to confirm the identity and purity of the solid products in comparison to literature data.

High-resolution powder XRD: Beamline ID31 of the European Synchrotron Radiation Facility (ESRF) was used to perform high resolution

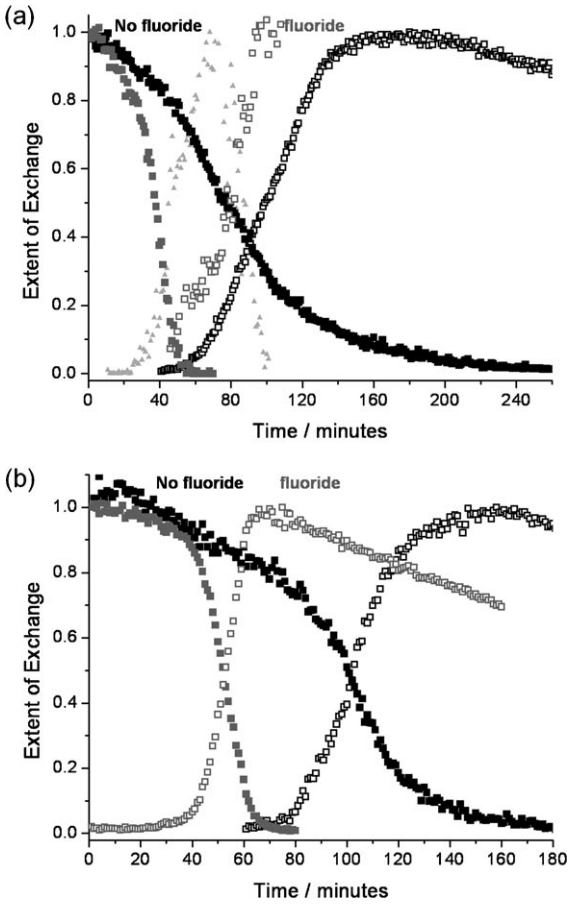

Figure 8. Comparison of kinetics of exchange for fluorinated (shown in grey) and purely hydroxylated (shown in black) MIL-53(Fe) for (a) propan-1-ol addition and (b) propan-2-ol addition. The starting material is represented by open squares, the fully open product as closed squares and the partially open intermediate (where seen) by filled triangles.

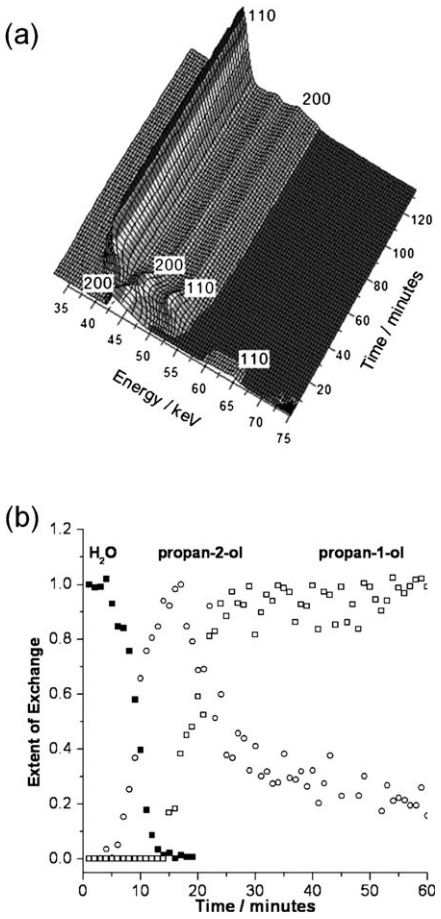

Figure 9. (a) Contour map of EDXRD measured during the addition of a 50:50 mixture of propan-1-ol and propan-2-ol to MIL-53(Fe,F,OH)[H_2O] where the detector angle was set at 1.50 °2θ. (b) Integration of peak intensities showing extent of guest exchange.

powder X-ray diffraction of the MIL-53(Fe) hosts and in the presence of various guest molecules. The beamline receives X-rays from the synchrotron source (which operates with an average energy of 6 GeV and a current beam of typically 100 mA) from an undulator device. The incident X-ray wavelength was 0.79989 Å and a beam size of 2.0 mm (horizontal) × 1.0 mm (vertical) was used. Samples were loaded into 1 mm diameter quartz capillaries. For the cases in which the interaction of samples with an organic guest was to be studied, the liquid solvent was injected into the capillary and the capillary then centrifuged to concentrate the solid to the end of sample holder; this minimised the background of the liquid and prevented the loss of solvent from the solid during the experiment. The samples were rapidly spun during data collection to ensure good powder averaging. Extraction of the peak positions, pattern indexing profile fitting analysis and Rietveld refinement were carried out with the TOPAS software.[22] Unit cells and space groups were found unambiguously by the LSI-Indexing method with satisfactory figures of merit and confirmed by pattern matching using the Le Bail method. In the case of MIL-53(Fe) immersed in a methanol and water mixture, the already published atomic coordinates of its partially expanded skeleton[20] were used as a starting model in the Rietveld refinement. The independent terephthalate ion was treated as a rigid body, and an anisotropic line broadening effect was corrected for by using a spherical harmonics series.[23] Although this allowed the structure of the framework to be refined and Fourier calculations showed the presence of electron density within the porous structure, location of the trapped methanol and/or water molecules was not possible. The same was true for the other alcohol guests, and we conclude that the alcohol molecules are highly disordered in these materials.

Time-resolved powder X-ray diffraction experiments: This paper includes results from two beamlines that were used to measure in situ EDXRD data from reactions between suspensions of solid MIL-53(Fe)[H_2O] and various organic alcohols in the liquid state, diluted where necessary with water (see below). The earlier results were obtained using Station 16.4[24] of the Daresbury SRS, UK (now permanently closed), while later experiments were performed using Beamline F3[25] of the HASYLAB facility at DESY, Hamburg, Germany. On Station 16.4, the incident beam was continuous over 5–120 keV, but after attenuation by the cell, X-ray energies of $>$ 30 keV have sufficient intensity to contribute to the EDXRD spectra. This beamline was equipped with a three-element solid-state germanium detector, with each detector separated by approximately 2 °2θ, to allow the simultaneous acquisition of three regions of diffraction patterns.[26] Beamline F3 receives white-beam radiation with energy 13.5–65 keV and the incident X-ray beam is collimated to dimensions $20 \times 20\ \mu m^2$. Scattered X-rays here are detected using a single-element germanium solid-state detector. For both beamlines the precise angle(s) of the detectors were calibrated using a set of Bragg peaks measured from a solid polycrystalline sample of MIL-53(Fe)[H_2O] and the energy calibration of the detector(s) was performed using a glass containing a series of heavy elements with well-separated fluorescence lines. Note that since the data were recorded during several visits to the beamlines, the

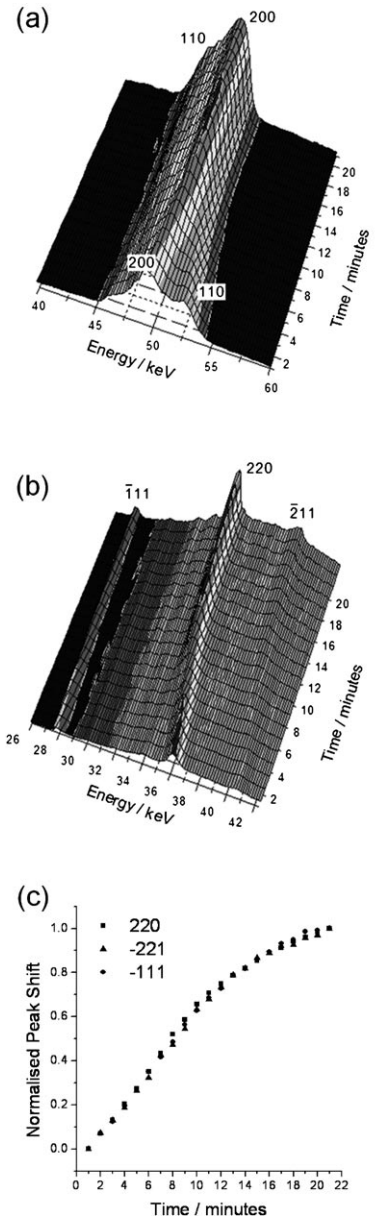

Figure 10. Contour maps of EDXRD measured during the addition of a 10% solution of pyridine in propan-2-ol to MIL-53(Fe,F,OH)[propan-2-ol] simultaneously measured from the detector at (a) 1.50 °2θ and (b) 4.39 °2θ. (c) Plots of normalised Bragg peak positions during the process.

detector angles were slightly different between each run and the detectors were always recalibrated on each visit.

In the EDXRD experiment the d-spacing (d/Å) of each characteristic Bragg peak is defined by an energy (E/keV), related to the fixed angle of the detector (2θ) by Equation (1).[27]

$$d = \frac{6.1992}{E \sin\theta} \quad (1)$$

In the experiments reported herein, around 400 mg of solid MIL-53(Fe)-[H_2O] was added to approximately 3 mL of deionised water in a 1 cm diameter borosilicate glass tube along with a Teflon-coated magnetic stirrer bar. Identical reaction tubes were used for both beamlines and the addition of alcohol guest molecules was made using a syringe pump with the tube placed in a stand equipped with a magnetic spinner. Data were accumulated in 60 s intervals with continuous stirring of the solid–liquid mixture whilst the guest solution (either pure alcohol or diluted with water) was added dropwise using an electronic syringe pump supplied by KD Scientific. The rate of addition of liquid to the suspension was varied between 10 and 1 mL per hour as described below. This controlled addition was necessary since the reaction was found to be very rapid: upon full addition of the organic guest solution and measurement of the diffraction data the reactions were found to already have reached completion. Although the addition of liquid by a syringe pump prevents the acquisition of true kinetic data, it has previously been used successfully to observe solid–liquid reactions that happen on short time-scales.[28] To check continuity between the data measured using the two beamlines, certain experiments were repeated on each instrument and the results were indeed found to be reproducible. Raw EDXRD data were converted using the programs DLConverter[29] and PowDLL[30] into a format suitable for reading into the program XFIT[31] where peak fitting using Pseudo-Voigt functions was undertaken to determine Bragg peaks areas and positions as a function of time to produce extent of reaction curves.

Acknowledgements

The research leading to these results has received funding from the European Community's Seventh Framework Programme (FP7/2007–2013) under grant agreement No. 228862. MACADEMIA is a Large-scale Integrating Project under the Nanosciences, Nanotechnologies, Materials and New Production Technologies Theme, which provided a studentship for A.S.M. We thank the STFC for provision of beamtime at the Daresbury SRS, ESRF for beamtime on ID31 and DESY for beamtime at HASYLAB. We are grateful to Dr. Andy Fitch of the ESRF for his assistance with running the experiments on ID31 and to Mark Feyand of the Christian-Albrechts-Universität zu Kiel for his assistance with use of Beamline F3 at HASYLAB.

[1] a) G. Férey, *Chem. Soc. Rev.* **2008**, *37*, 191; b) J. R. Long, O. M. Yaghi, *Chem. Soc. Rev.* **2009**, *38*, 1213–1214; c) L. R. MacGillivray, *Metal-Organic Frameworks: Design and Application*, Wiley, New York, **2010**; d) C. J. Kepert in *Inorganic Materials Series: Porous Materials.* (Eds.: D. O'Hare, D. W. Bruce, R. I. Walton), Wiley, New York, **2010**.

[2] a) R. M. Barrer, *Zeolites and Clay Minerals as Sorbents and Molecular Sieves*, Academic Press, London, **1978**; b) R. Xu, W. Peng, J. Yu, Q. Huo, J. Chen, *Chemistry of Zeolites and Related Porous Materials*, Wiley, New York, **2007**; c) J. Cejka, H. van Bekkum, A. Corma, F. Schuth, *Studies in Surface Science and Catalysis, Vol. 168, Introduction to Zeolite Science and Practise*, 3rd ed., Elsevier, Amsterdam **2007**.

[3] a) O. M. Yaghi, M. O'Keeffe, N. W. Ockwig, H. K. Chae, M. Eddaoudi, J. Kim, *Nature* **2003**, *423*, 705; b) M. O'Keeffe, *Chem. Soc. Rev.* **2009**, *38*, 1215.

[4] a) Z. Wang, S. M. Cohen, *Chem. Soc. Rev.* **2009**, *38*, 1315; b) H. Sato, R. Matsuda, K. Sugimoto, M. Takata, S. Kitagawa, *Nat. Mater.* **2010**, *9*, 661–666.

[5] a) A. J. Fletcher, K. M. Thomas, M. J. Rosseinsky, *J. Solid State Chem.* **2005**, *178*, 2491–2510; b) G. Férey, C. Serre, *Chem. Soc. Rev.* **2009**, *38*, 1380.

[6] A. U. Czaja, N. Trukhan, U. Müller, *Chem. Soc. Rev.* **2009**, *38*, 1284.

[7] a) S. S. Han, J. L. Mendoza-Cortés, W. A. Goddard, *Chem. Soc. Rev.* **2009**, *38*, 1460; b) L. J. Murray, M. Dinc, J. R. Long, *Chem. Soc. Rev.* **2009**, *38*, 1294.

[8] a) J. Lee, O. K. Farha, J. Roberts, K. A. Scheidt, S. T. Nguyen, J. T. Hupp, *Chem. Soc. Rev.* **2009**, *38*, 1450–1459; b) J.-R. Li, R. J. Kuppler, H.-C. Zhou, *Chem. Soc. Rev.* **2009**, *38*, 1477; c) L. Ma, C. Abney, W. Lin, *Chem. Soc. Rev.* **2009**, *38*, 1248.

[9] G. Férey, F. Millange, M. Morcrette, C. Serre, M. L. Doublet, J. M. Grenèche, J. M. Tarascon, *Angew. Chem.* **2007**, *119*, 3323; *Angew. Chem. Int. Ed.* **2007**, *46*, 3259.
[10] P. Horcajada, C. Serre, G. Maurin, N. A. Ramsahye, F. Balas, M. Vallet-Regi, M. Sebban, F. Taulelle, G. Férey, *J. Am. Chem. Soc.* **2008**, *130*, 6774–6780.
[11] K. Uemura, R. Matsuda, S. Kitagawa, *J. Solid State Chem.* **2005**, *178*, 2420–2429.
[12] a) T. K. Maji, R. Matsuda, S. Kitagawa, *Nat. Mater.* **2007**, *6*, 142–148; b) S. Noro, D. Tanaka, H. Sakamoto, S. Shimomura, S. Kitagawa, S. Takeda, K. Uemura, H. Kita, T. Akutagawa, T. Nakamura, *Chem. Mater.* **2009**, *21*, 3346–3355; c) S. Shimomura, M. Higuchi, R. Matsuda, K. Yoneda, Y. Hijikata, Y. Kubota, Y. Mita, J. Kim, M. Takata, S. Kitagawa, *Nat. Chem.* **2010**, *2*, 633–637.
[13] J. Rabone, Y. F. Yue, S. Y. Chong, K. C. Stylianou, J. Bacsa, D. Bradshaw, G. R. Darling, N. G. Berry, Y. Z. Khimyak, A. Y. Ganin, P. Wiper, J. B. Claridge, M. J. Rosseinsky, *Science* **2010**, *329*, 1053–1057.
[14] a) C. Serre, F. Millange, S. Surble, G. Férey, *Angew. Chem. Int. Ed.* **2004**, *43*, 6285; b) C. Serre, C. Mellot-Draznieks, S. Surblé, N. Audebrand, Y. Filinchuk, G. Férey, *Science* **2007**, *315*, 1828.
[15] a) F. Millange, C. Serre, G. Férey, *Chem. Commun.* **2002**, 822; b) C. Serre, F. Millange, C. Thouvenot, M. Nogues, G. Marsolier, D. Louer, G. Férey, *J. Am. Chem. Soc.* **2002**, *124*, 13519; c) F. Millange, N. Guillou, R. I. Walton, J. M. Greneche, I. Margiolaki, G. Férey, *Chem. Commun.* **2008**, 4732–4734; d) I. Beurroies, M. Boulhout, P. L. Llewellyn, B. Kuchta, G. Férey, C. Serre, R. Denoyel, *Angew. Chem.* **2010**, *122*, 7688–7691; *Angew. Chem. Int. Ed.* **2010**, *49*, 7526–7529.
[16] a) G. Férey, M. Latroche, C. Serre, F. Millange, T. Loiseau, A. Percheron-Guegan, *Chem. Commun.* **2003**, 2976–2977; b) P. L. Llewellyn, S. Bourrelly, C. Serre, Y. Filinchuk, G. Férey, *Angew. Chem.* **2006**, *118*, 7915; *Angew. Chem. Int. Ed.* **2006**, *45*, 7751; c) C. Serre, S. Bourrelly, A. Vimont, N. A. Ramsahye, G. Maurin, P. L. Llewellyn, M. Daturi, Y. Filinchuk, O. Leynaud, P. Barnes, G. Férey, *Adv. Mater.* **2007**, *19*, 2246; d) N. A. Ramsahye, G. Maurin, S. Bourrelly, P. L. Llewellyn, T. Loiseau, C. Serre, G. Férey, *Chem. Commun.* **2007**, 3261; e) P. L. Llewellyn, G. Maurin, T. Devic, S. Loera-Serna, N. Rosenbach, C. Serre, S. Bourrelly, P. Horcajada, Y. Filinchuk, G. Férey, *J. Am. Chem. Soc.* **2008**, *130*, 12808–12814; f) T. K. Trung, P. Trens, N. Tanchoux, S. Bourrelly, P. L. Llewellyn, S. Loera-Serna, C. Serre, T. Loiseau, F. Fajula, G. Férey, *J. Am. Chem. Soc.* **2008**, *130*, 16926–16932; g) F. Salles, D. I. Kolokolov, H. Jobic, G. Maurin, P. L. Llewellyn, T. Devic, C. Serre, G. Férey, *J. Phys. Chem. C* **2009**, *113*, 7802–7812; h) L. Hamon, P. L. Llewellyn, T. Devic, A. Ghoufi, G. Clet, V. Guillerm, G. D. Pirngruber, G. Maurin, C. Serre, G. Driver, W. van Beek, E. Jolimaitre, A. Vimont, M. Daturi, G. Férey, *J. Am. Chem. Soc.* **2009**, *131*, 17490–17499; i) L. Hamon, C. Serre, T. Devic, T. Loiseau, F. Millange, G. Férey, G. De Weireld, *J. Am. Chem. Soc.* **2009**, *131*, 8775; j) S. Bourrelly, B. Moulin, A. Rivera, G. Maurin, S. Devautour-Vino, C. Serre, T. Devic, P. Horcajada, A. Vimont, G. Clet, M. Daturi, J. C. Lavalley, S. Loera-Serna, R. Denoyel, P. L. Llewellyn, G. Férey, *J. Am. Chem. Soc.* **2010**, *132*, 9488–9498; k) S. Devautour-Vinot, G. Maurin, F. Henn, C. Serre, G. Férey, *Phys. Chem. Chem. Phys.* **2010**, *12*, 12478–12485.
[17] C. Volkringer, T. Loiseau, N. Guillou, G. Férey, E. Elkaim, A. Vimont, *Dalton Trans.* **2009**, 2241–2249.
[18] F. Millange, C. Serre, N. Guillou, G. Férey, R. I. Walton, *Angew. Chem.* **2008**, *120*, 4168; *Angew. Chem. Int. Ed.* **2008**, *47*, 4100.
[19] a) J. Munn, P. Barnes, D. Hausermann, S. A. Axon, J. Klinowski, *Phase Transitions* **1992**, *39*, 129; b) R. J. Francis, S. J. Price, J. S. O. Evans, S. O' Brien, D. O'Hare, S. M. Clark, *Chem. Mater.* **1996**, *8*, 2102; c) R. J. Francis, S. O'Brien, A. M. Fogg, P. S. Halasyamani, D. O'Hare, T. Loiseau, G. Férey, *J. Am. Chem. Soc.* **1999**, *121*, 1002; d) R. I. Walton, T. Loiseau, D. O'Hare, G. Férey, *Chem. Mater.* **1999**, *11*, 3201; e) P. Barnes, S. Colston, B. Craster, C. Hall, A. Jupe, S. Jacques, J. Cockcroft, S. Morgan, M. Johnson, D. O'Connor, M. Bellotto, *J. Synchrotron Radiat.* **2000**, *7*, 167; f) R. I. Walton, D. O'Hare, *Chem. Commun.* **2000**, 2283; g) R. I. Walton, F. Millange, D. O'Hare, A. T. Davies, G. Sankar, C. R. A. Catlow, *J. Phys. Chem. B* **2001**, *105*, 83; h) R. Kiebach, M. Schaefer, F. Porsch, W. Bensch, *Z. Anorg. Allg. Chem.* **2005**, *631*, 369–374; i) R. Kiebach, N. Pienack, M. E. Ordolff, F. Studt, W. Bensch, *Chem. Mater.* **2006**, *18*, 1196; j) N. Yee, S. Shaw, L. G. Benning, T. H. Nguyen, *Am. Mineral.* **2006**, *91*, 92; k) M. G. O'Brien, M. Sanchez-Sanchez, A. M. Beale, D. W. Lewis, G. Sankar, C. R. A. Catlow, *J. Phys. Chem. C* **2007**, *111*, 16951–16961; l) G. Sankar, T. Okubo, W. Fan, F. Meneau, *Faraday Discuss.* **2007**, *136*, 157; m) R. Kiebach, N. Pienack, W. Bensch, J. D. Grunwaldt, A. Michailovski, A. Baiker, T. Fox, Y. Zhou, G. R. Patzke, *Chem. Mater.* **2008**, *20*, 3022; n) D. R. Modeshia, R. J. Darton, S. E. Ashbrook, R. I. Walton, *Chem. Commun.* **2009**, 68–70.
[20] F. Millange, N. Guillou, M. E. Medina, G. Férey, A. Carlin-Sinclair, K. M. Golden, R. I. Walton, *Chem. Mater.* **2010**, *22*, 4237–4245.
[21] Note that all Bragg peaks for each phase grow and/or decay in the same manner, proved by integration of several observed peaks, see the Supporting Information.
[22] Topas V4.2: General Profile and Structure Analysis Software for Powder Diffraction Data, Bruker AXS Ltd., **2004**.
[23] L. W. Finger, D. E. Cox, A. P. Jephcoat, *J. Appl. Crystallogr.* **1994**, *27*, 892.
[24] S. M. Clark, *Nucl. Instrum. Methods Phys. Res. Sect. A* **1996**, *381*, 161–168.
[25] J. S. Olsen, B. Buras, L. Gerward, S. Steenstrup, *J. Phys. E* **1981**, *14*, 1154–1158.
[26] G. Muncaster, A. T. Davies, G. Sankar, C. R. A. Catlow, J. M. Thomas, S. L. Colston, P. Barnes, R. I. Walton, D. O'Hare, *Phys. Chem. Chem. Phys.* **2000**, *2*, 3523.
[27] B. C. Giessen, G. E. Gordon, *Science* **1968**, *159*, 973.
[28] D. O'Hare, J. S. O. Evans, A. Fogg, S. O'Brien, *Polyhedron* **2000**, *19*, 297.
[29] M. Smith, S. Gontier, *DlConverter 1.3*, Daresbury Laboratory, Warrington, **1999**.
[30] N. Kourkoumelis, PowDLL: A program for the interconversion of powder diffraction data files Version 2.19, University of Ioannina, Ioannina, **2009**, http://users.uoi.gr/nkourkou/powdll.htm.
[31] R. W. Cheary, A. A. Coelho, *Program XFIT*, deposited in CCP14 Powder Diffraction Library, Engineering and Physical Sciences Research Council, Daresbury Laboratory, Warrington, **1996**, http://www.ccp14.ac.uk/.

Received: December 16, 2010
Published online: May 9, 2011

